

Creation of Fluorescent RXR Antagonists Based on CBTF-EE and Application to a Fluorescence Polarization Binding Assay

Maho Takioku,[#] Yuta Takamura,[#] Michiko Fujihara, Masaki Watanabe, Shoya Yamada, Mayu Kawasaki, Sohei Ito, Shogo Nakano, and Hiroki Kakuta*Cite This: *ACS Med. Chem. Lett.* 2021, 12, 1024–1029

Read Online

ACCESS |



Metrics & More



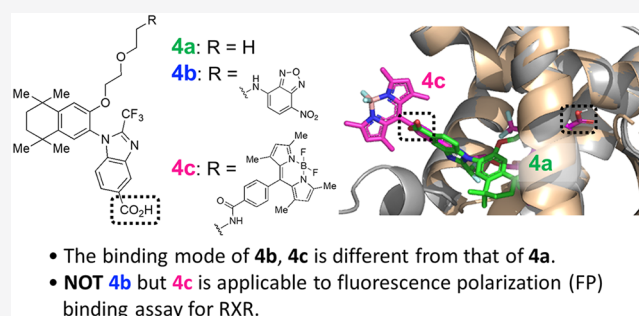
Article Recommendations



Supporting Information

ABSTRACT: Retinoid X receptor (RXR) ligands often bind in modes in which the carboxy group forms a hydrogen bond inside the ligand-binding pocket (LBP). However, our previously reported RXR antagonist, CBTF-EE (**4a**), binds with its carboxy group directed outside the LBP and its alkoxy side chain located inside the LBP. Here, we examined the binding modes of **4b** and **4c** bearing a nitrobenzoxadiazole (NBD) or boron-dipyrromethene (BODIPY) fluorophore, respectively, at the end of the alkoxy chain of **4a**. Both compounds function as RXR antagonists. **4c**, but not **4b**, was available for a fluorescence polarization binding assay, indicating that rotation of BODIPY, but not NBD, is restricted in the bound state. The fluorescence findings, supported by docking simulations, suggest the fluorophores are located outside the LBP, so that the binding mode of **4b** and **4c** is different from that of **4a**. The assay results were highly correlated with those of a [³H]9-*cis*-retinoic acid assay.

KEYWORDS: RXR, fluorescence, NBD, BODIPY, fluorescence polarization, binding assay



The World Health Organization (WHO) predicts that lifestyle-related diseases such as ischemic heart disease, stroke, and chronic obstructive pulmonary disease (COPD) will account for a large proportion of the world's causes of death in the 21st century.¹ Such lifestyle-related diseases are related to lack of exercise as well as obesity and arteriosclerosis, which in turn are associated with excessive intake of high-fat diets and smoking.² These diseases are generally treated with drugs that target specific proteins. For example, calcium-channel blockers and adrenaline β -blockers are used to treat ischemic heart disease, while antithrombotic drugs such as cyclooxygenase inhibitors are used to treat stroke, and anticholinergic drugs and β -stimulators that induce bronchodilation are used to treat COPD. However, as these diseases are caused by multiple factors in vivo, there is also interest in the approach used in traditional oriental medicine, such as Chinese medicine, which aims to broadly improve homeostasis in the body. We considered that if such a broadly based improvement of homeostasis could be achieved using a molecular-targeted drug, then this might be an effective approach to reduce the number of different drugs taken by patients. We call this idea "Western-style Chinese medicine". With this idea in mind, we have focused on retinoid X receptors (RXRs),³ because it is well-known that RXRs function in concert with a variety of other nuclear receptors.

RXRs are members of the nuclear receptor superfamily and regulate the transcription of downstream genes in response to

ligand binding.⁴ Although RXR homodimers exist, their function remains unclear.^{5,6} On the other hand, RXR heterodimers with other nuclear receptors, such as peroxisome proliferator-activated receptor (PPAR), thyroid hormone receptor (TR), and liver X receptor (LXR), are key players in the regulation of the internal body environment.^{5,6} In particular, PPAR/RXR and LXR/RXR are reported to be allosterically activated by an RXR agonist alone, a phenomenon called the permissive effect.⁷ Bexarotene (**1**, Figure 1),⁸ which is clinically used to treat cutaneous T-cell lymphoma (CTCL), is an RXR agonist that activates these permissive RXR heterodimers.⁷ The effectiveness of RXR agonists for lifestyle-related diseases has also been reported, underlining the in vivo diversity of RXR function.^{9–11} Interestingly, therapeutic effects of RXR antagonists in an animal model of type 2 diabetes¹² and on viral infection in vitro¹³ have also been reported.

The representative RXR antagonist PA452 (**2**) inhibits not only RXR homodimers but also RXR heterodimers activated by partner receptor agonists.^{14–16} This means that RXR

Received: April 8, 2021

Accepted: May 5, 2021

Published: May 7, 2021



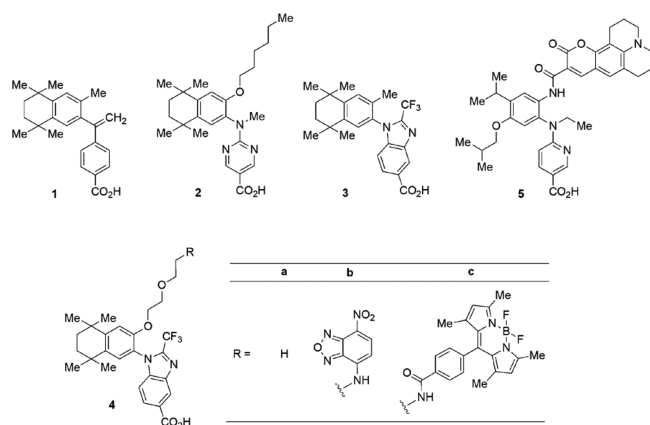


Figure 1. Chemical structures of RXR agonists **1** and **3** and antagonists **2**, **4**, and **5**.

antagonists of this type induce an “allosteric effect” that influences the partner receptor in the permissive RXR heterodimers. We were interested in RXR antagonists that do not show such allosteric inhibition but that effectively inhibit RXR homodimers. Based on the observation that allosteric activation of PPAR γ /RXR, a permissive RXR heterodimer, by CBTF-PMN (**3**) is weak,¹⁷ we designed a nonallosteric RXR antagonist, CBTF-EE (**4a**), and confirmed that it does not show allosteric inhibition of permissive RXR heterodimers, in contrast to **2**.¹⁸ One reason for this difference is thought to be the binding mode of **4a** in the human RXR α ligand-binding pocket (hRXR α -LBP). Most reported RXR ligands bind in modes in which the carboxy group enters the LBP, whereas our X-ray cocrystal analysis indicated that the carboxy group of **4a** is directed outside the hRXR α -LBP, and instead, the alkoxy chain is located inside the LBP.¹⁸ In addition, an AutoDock docking simulation of our previously reported fluorescent RXR antagonist NET-C343 (**5**) suggested that **5** has a similar binding mode to **4a**, i.e., that the fluorophore coumarin 343 (C343), not the carboxy group, enters the LBP.¹⁹

Consequently, we were interested to see whether the introduction of a fluorescent group at the end of the alkoxy chain of **4a** would afford fluorescent RXR-antagonistic derivatives whose fluorophore would enter the LBP. Compounds that show changes in fluorescence properties in response to a change in the environment or a decrease in molecular motility are expected to be applicable for RXR ligand-binding assays. Thus, in this study, we designed and synthesized derivatives of **4a** bearing a fluorescent group at the end of the alkoxy side chain and evaluated their RXR antagonist activities and fluorescence properties.

As fluorophores, we selected nitrobenzoxadiazole (NBD) and boron-dipyrrromethene (BODIPY), which have fairly similar excitation and fluorescence wavelengths^{20,21} that are longer than those of fluorescence amino acids such as tyrosine and tryptophan present in RXR and can be detected by a fluorescent plate reader using readily available filters. Furthermore, NBD is a relatively small molecule, while BODIPY is sterically bulky. The size of the fluorophore is likely to affect its ability to enter the LBP.

Compounds **4b** (bearing NBD) and **4c** (bearing BODIPY) were obtained by linking NBD-Cl or carboxy-BODIPY via an amino group (SI Schemes S1 and S2). A reporter gene assay using COS-1 cells revealed that both **4b** and **4c** act as RXR

antagonists, although they are less potent than **4a** (Figure 2B). The fluorescence properties in MeOH solution were evaluated,

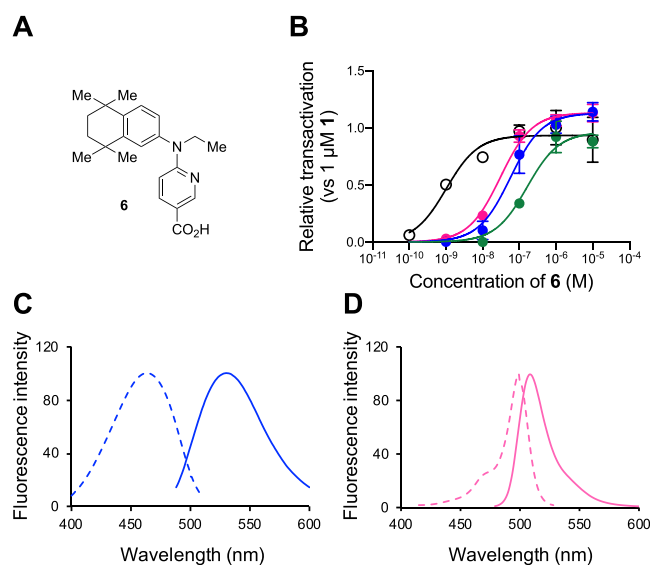


Figure 2. RXR-antagonistic activity and fluorescence properties of **4b** and **4c**. (A) Chemical structure of NET-TMN (**6**), an RXR agonist.²² (B) Antagonistic activities of **4a–4c** toward hRXR α homodimer in COS-1 cells. Transactivation of **6** (open circles) relative to DMSO in the absence or presence of 1 μ M **4a** (green), **4b** (blue), or **4c** (pink). Data are mean \pm SD ($n = 3$). (C,D) Fluorescence excitation spectra (broken line) and emission spectra (solid line) of 1 μ M **4b** (C) and **4c** (D) in MeOH solution, respectively.

and the excitation (λ_{Ex})/fluorescence (λ_{Em}) maxima of **4b** and **4c** were 464 nm/530 nm and 499 nm/509 nm, respectively (Figure 2C,D and Table 1). The molar extinction coefficient

Table 1. Fluorescence Properties of **4b** and **4c**

compd	solvent	ϵ [L/(mol·cm)]	λ_{Ex} [nm]	λ_{Em} [nm]	Φ^a
4b	MeOH	6.7×10^3	464	530	0.224 ± 0.05
	EtOH	8.4×10^3	461	527	0.237 ± 0.03
4c	MeOH	2.8×10^4	499	508	0.349 ± 0.01
	EtOH	2.8×10^4	499	509	0.471 ± 0.04

^aData are mean \pm SD ($N = 3$). ^bStandard compound: coumarin 6 ($\lambda_{\text{Ex}} = 459$ nm, $\Phi = 0.78$).²³

(ϵ) and the fluorescence quantum yield (Φ) of **4c** were both slightly larger than those of **4b**. A similar tendency was also observed in EtOH (Table 1).

Ligand binding to the hRXR α -LBD quenches the fluorescence around $\lambda_{\text{Em}} = 330$ nm due to Trp282 and Trp305 in the LBD via FRET, and binding assays based on this phenomenon can be used to determine the K_d values.^{24,25} Concentration-dependent quenching around $\lambda_{\text{Em}} = 330$ nm was observed at $\lambda_{\text{Ex}} = 290$ nm (Figure 3A,B), and the K_d values of **4b** and **4c** were obtained as 0.629 ± 0.074 and 0.761 ± 0.057 μ M ($N = 3$, mean \pm SD), respectively. As regarding the fluorescence derived from each fluorophore, the fluorescence intensity of **4b** at 550 nm and that of **4c** at 520 nm increased in a concentration-dependent manner (Figure 3A,B). The fluorescence intensity also increased in response to excitation at the maximum excitation wavelength of each compound (SI Figure S1). **4c** showed a high correlation between quenching at

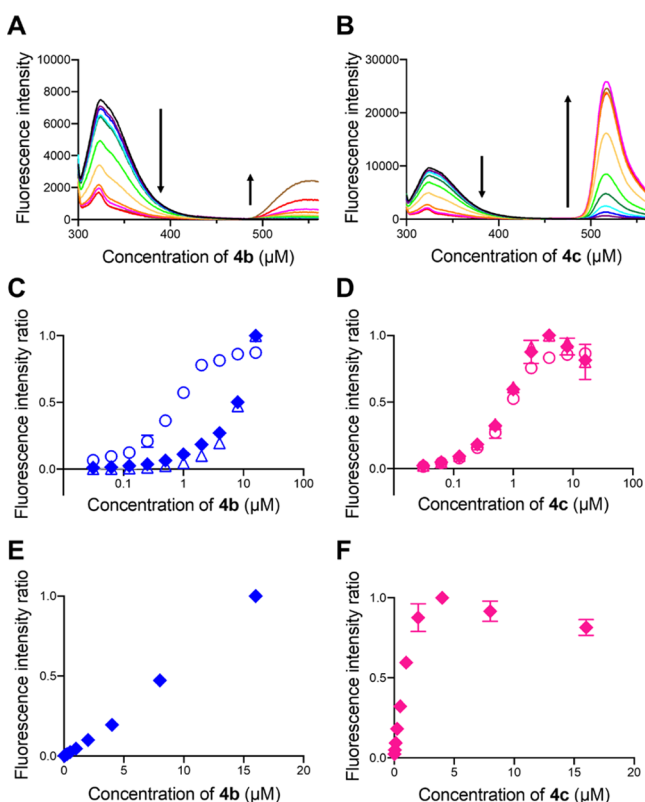


Figure 3. Fluorescence spectra and intensity ratios of **4b** or **4c** in the absence and presence of hRXR α -LBD. (A,B) Fluorescence titration emission spectra of hRXR α -LBD (0.5 μ M) upon addition to (A) **4b** or (B) **4c** (0–16 μ M, black–brown) in HEPES buffer at $\lambda_{\text{Ex}} = 290$ nm. (C,D) Fluorescence intensity ratios [$1 - F_{330 \text{ nm}}/F_{330 \text{ nm}}$] ($\lambda_{\text{Ex}} = 290$ nm/ $\lambda_{\text{Em}} = 330$ nm, open circles) and [$F_{550 \text{ nm}}/F_{550 \text{ nm}}$] (**4b**; $\lambda_{\text{Ex}} = 290$ nm/ $\lambda_{\text{Em}} = 550$ nm, open triangles; $\lambda_{\text{Ex}} = 478$ nm/ $\lambda_{\text{Em}} = 550$ nm, closed diamonds) or [$F_{520 \text{ nm}}/F_{520 \text{ nm}}$] (**4c**; $\lambda_{\text{Ex}} = 290$ nm/ $\lambda_{\text{Em}} = 520$ nm, open triangles; $\lambda_{\text{Ex}} = 502$ nm/ $\lambda_{\text{Em}} = 520$ nm, closed diamonds). F_0 and F are the fluorescence intensity in the absence of **4b** or **4c** at each wavelength and the observed fluorescence intensity, respectively. (E,F) Replots of selected data from (C,D) on a linear scale.

330 nm and increasing fluorescence intensity near 520 nm, but **4b** did not (Figure 3C–F).

Since the fluorescence intensity of **4c** increased in response to binding to the hRXR α -LBD, it was expected that the fluorescence intensity would decrease due to competition in the presence of RXR ligands. However, although there appeared to be competition between **4c** and **1** after incubation for 1 h, there was significant variability in the data (Figure 4A). A similar tendency was seen upon incubation for 0 or 2 h (SI Figure S2A). Therefore, we decided to examine the fluorescence polarization instead. Fluorescence polarization is considered to be due to a reduction of the mobility of the fluorescence label upon binding to a receptor having a large molecular weight.^{26,27} When changes in the fluorescence polarization of **4c** in the presence of various concentrations of hRXR α -LBD were investigated, stable and reproducible results were obtained (Figure 4B). Interestingly, competition between **4b** and **1** could not be observed (SI Figure S2C). The fact that the fluorescence polarization of **4b** was unaffected in the presence of the hRXR α -LBD indicates that the motility of the NBD fluorophore is not affected by binding of **4b** to the hRXR α -LBD. This in turn suggests that the fluorophore at the end of the alkoxy chain of **4b** exists outside the LBP. Since

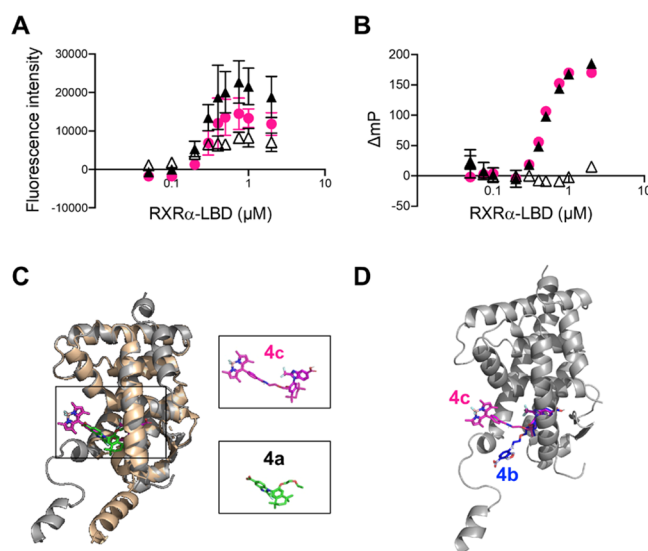


Figure 4. Fluorescence change upon binding with hRXR α -LBD and docking study. (A) Fluorescence intensity and (B) fluorescence polarization data for **4c** (0.3 μ M) at $\lambda_{\text{Ex}} = 485$ nm/ $\lambda_{\text{Em}} = 535$ nm. The saturation curve (pink circles) was calculated by subtracting “with 10 μ M **1** (open triangles)” from “without **1** (closed triangles)”. Data are mean \pm SD ($N = 3$). The K_d value of **4c** for the hRXR α -LBD was obtained as 0.375 ± 0.134 μ M from curve fitting of the dose-dependent saturation curves (pink). (C) Comparison of the binding mode of **4c** (pink) to hRXR α -LBD (PDB code: 3A9E,³⁰ gray) predicted by AutoDock with that in the X-ray cocrystal structure of **4a** (green) with the hRXR α -LBD (PDB code: 7CFO,¹⁸ pale orange). (D) Predicted binding modes of **4b** (blue) and **4c** (pink) in the antagonistic form with hRXR α -LBD (PDB code: 3A9E³⁰). The fluorophore is located outside the LBP in both cases.

NBD is structurally small and has low lipophilicity, it seems likely that a “propeller effect”²⁸ occurs, i.e., NBD can rotate freely like a propeller in the solvent outside the LBP. The BODIPY moiety of **4c** is larger than NBD and so should also be located outside the hRXR α -LBD. However, the larger size of BODIPY compared to NBD may mean that the BODIPY moiety of **4c** can nevertheless not rotate freely, and consequently, fluorescence polarization is observed. Docking simulations on AutoDock Vina²⁹ were performed using an X-ray structure of the RXR-antagonistic form. For **4c**, since AutoDock vina does not support the B atom, the structure other than the fluorophore (**S1**, SI Figure S3) was separated from the fluorophore (**S2**, SI Figure S3) using Chem3D. These structures and **4b** were energetically minimized by means of molecular mechanics (MM) and semiempirical molecular orbital calculations (MOPAC, PM3 for **S1** and **6c**, and AM1 for **S2**). When we used the hRXR α -LBD coordinates (PDB code: 7CFO¹⁸) obtained from the X-ray analysis of the cocrystal with **4a**, docking simulation with **S1** or **4c** failed. The reason for this is thought to be that the space occupied by the alkoxy side chain of **4a** is too narrow to accept the benzamide moiety of **S1** or NBD. Docking simulation using the hRXR α -LBD coordinates obtained from the X-ray analysis of the cocrystal with RXR antagonist LG100754 (**S3**, SI Figure S3),³⁰ which has a wider ligand-binding pocket (LBP), was successful. For **4c**, the lowest-energy structure of **S1** was combined with **S2**. The obtained binding mode seems reasonable, although a cocrystal structure analysis will be needed to enable detailed discussion. The docking data show that **4b** or **4c** binds in modes in which the carboxy group forms a hydrogen bond

inside the LBP and each fluorophore is located outside the LBP, whereas the carboxylic acid moiety of **4a** is located outside the LBP (Figure 4C,D and SI movies S1 and S2). These results support the binding modes of **4b** and **4c** inferred from the fluorescence findings.

Since the above results indicate that **4c** could be used for a fluorescence-polarization-based RXR ligand-binding assay, we set out to identify suitable conditions. Figure 4B shows the results obtained with a fixed concentration of 0.3 μM **4c**. We also tried 0.1 μM **4c**, but the baseline was higher, and the change in fluorescence polarization (ΔmP) was smaller (SI Figure S2B). There was no significant difference in incubation time between 1 and 2 h (SI Figure S2B). We also examined the time-dependent change of the Z' factor as a measure of the quality of the screening³¹ and found that it was >0.6 at both time points, indicating that this assay is stable. As regarding the receptor concentration, a receptor concentration at which 50–80% of the receptors are in the bound state is appropriate for the ligand-binding assay.³² Thus, the hRXR α -LBD concentration should be 0.5 to 1 μM when 0.3 μM **4c** is used (SI Figure S2B). Finally, we selected 0.3 μM **4c**, 0.5 μM hRXR α -LBD, and a 1 h incubation time as the optimum conditions and examined the change in fluorescence polarization at various concentrations of test compound **1**. A concentration-dependent decrease of fluorescence polarization was observed (Figure 5A), and the IC_{50} was obtained as 632 ± 103 nM (mean \pm SD, $N = 3$). The K_i value was calculated as 350 nM using the Cheng–Prusoff equation³³ (the K_d value of **4c** is 375

nM as mentioned in Figure 4). The K_i value of **1** determined with the widely used [^3H]9-*cis* retinoic acid assay was 201 nM. Therefore, we next evaluated the binding abilities of various other RXR ligands (Figure 5C) under the same conditions. There was a high correlation between the obtained K_i values and those in the [^3H]9-*cis* retinoic acid assay ($R^2 = 0.9614$) (Figure 5B, SI Table S1, and SI Figure S4).

In conclusion, based on our previous finding that the alkoxy chain of RXR antagonist **4a** is located inside the RXR-LBP, we designed **4b** and **4c** bearing the fluorophores NBD and BODIPY, respectively, at the end of the alkyl chain. Although **4b** and **4c** both showed RXR antagonist activity, an increase in fluorescence polarization was observed only for **4c** in response to binding to the hRXR α -LBD, despite the fact that NBD is smaller than BODIPY. The fluorescence findings suggest that the fluorophore of **4b** and **4c** lies outside the LBD, unlike the alkyl chain of **4a**. Thus, the binding mode of **4b** or **4c** is different from that of **4a**. Docking calculations were consistent with this conclusion. Nevertheless, presumably because of restricted rotation of the large BODIPY moiety outside the LBP, **4c** could be used to evaluate the binding abilities of RXR ligands by means of a fluorescence polarization assay. The K_i values of various RXR ligands obtained in the optimized assay using **4c** were highly correlated with those obtained with the widely employed radioisotope method. Our assay enables convenient screening of retinoids within a few hours, without the need for processes such as filtration or precautions associated with the use of a radiolabel.

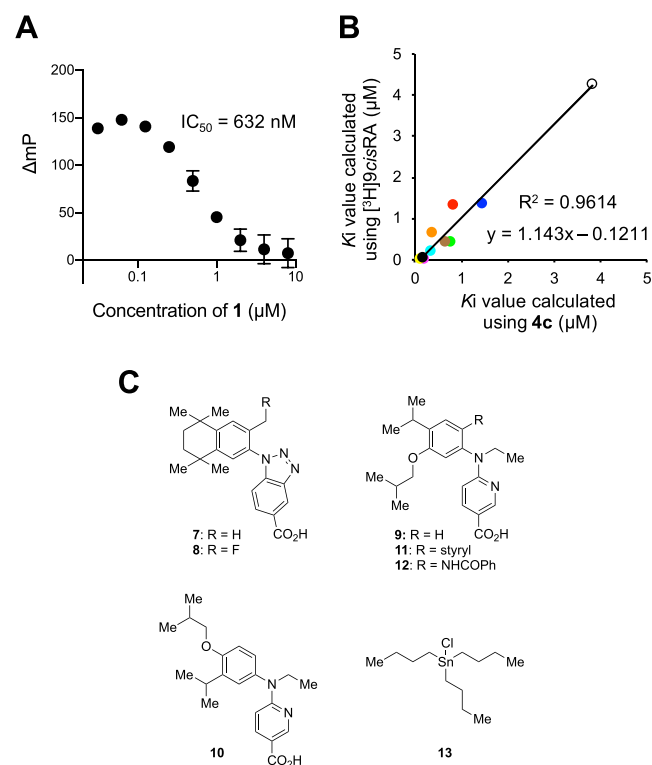


Figure 5. (A) Fluorescence polarization plot for **1** using **4c** at $\lambda_{\text{Ex}} = 485$ nm/ $\lambda_{\text{Em}} = 535$ nm. Data are mean \pm SD ($N = 3$). (B) Correlation of K_i values between this assay and the [^3H]9-*cis* retinoic acid assay. Light blue, bexarotene (**1**); red, PA452 (**2**); green, CBTF-PMN (**3**); blue, CBTF-EE (**4a**); yellow, NEt-TMN (**6**); white, CBt-PMN (**7**); pink, NEt-3IB (**9**); black, NEt-SB (**11**); brown, NEt-BA (**12**); and orange, TBtCl (**13**). (C) Chemical structures of the test compounds.

■ ASSOCIATED CONTENT

Supporting Information

The Supporting Information is available free of charge at <https://pubs.acs.org/doi/10.1021/acsmchemlett.1c00201>.

Experimental section, chemistry (preparation of RXR ligands, compound data), in vitro assay (luciferase reporter gene assay, UV-vis and fluorescence spectra measurements, determination of fluorescence quantum yield, cloning, expression, and purification of ligand-binding domain of RXR α , fluorescence titration measurements, fluorescence competition measurements, fluorescence polarization binding assay using **4c**, calculation of Z' -factor), docking simulation using AutoDock vina, synthetic schemes, figures (fluorescence spectra of **4b** and **4c**, fluorescence binding assay data, chemical structures for prediction of binding mode of **4c**, fluorescence polarization ratio curve of each compound using **4c**), table for K_i values of test compounds, NMR charts, MS charts, HPLC charts, and supporting movie legends (PDF)

Structural comparison of hRXR α -LBD/**4a** (PDB code: 7CFO) and a binding model of **4c** in the antagonistic form with hRXR α -LBD (PDB code: 3A9E) obtained with AutoDock vina (MOV)

Binding models of **4b** and **4c** in the antagonistic form with hRXR α -LBD (PDB code: 3A9E) obtained with AutoDock vina (MOV)

Molecular formula strings (XLSX)

■ AUTHOR INFORMATION

Corresponding Author

Hiroki Kakuta – Division of Pharmaceutical Sciences, Okayama University Graduate School of Medicine, Dentistry

and Pharmaceutical Sciences, Okayama 700-8530, Japan;
orcid.org/0000-0002-3633-8121; Phone: +81-(0)86-251-7963; Email: kakuta-h@okayama-u.ac.jp

Authors

Maho Takioku – Division of Pharmaceutical Sciences, Okayama University Graduate School of Medicine, Dentistry and Pharmaceutical Sciences, Okayama 700-8530, Japan

Yuta Takamura – Division of Pharmaceutical Sciences, Okayama University Graduate School of Medicine, Dentistry and Pharmaceutical Sciences, Okayama 700-8530, Japan;
orcid.org/0000-0001-9799-7123

Michiko Fujihara – Division of Pharmaceutical Sciences, Okayama University Graduate School of Medicine, Dentistry and Pharmaceutical Sciences, Okayama 700-8530, Japan; AIBIOS Co. Ltd., Tokyo 106-0032, Japan

Masaki Watanabe – Division of Pharmaceutical Sciences, Okayama University Graduate School of Medicine, Dentistry and Pharmaceutical Sciences, Okayama 700-8530, Japan;
orcid.org/0000-0003-1061-2679

Shoya Yamada – Division of Pharmaceutical Sciences, Okayama University Graduate School of Medicine, Dentistry and Pharmaceutical Sciences, Okayama 700-8530, Japan; Research Fellowship Division, Japan Society for the Promotion of Science, Tokyo 102-8472, Japan

Mayu Kawasaki – Graduate School of Integrated Pharmaceutical and Nutritional Sciences, University of Shizuoka, Shizuoka 422-8526, Japan

Sohei Ito – Graduate School of Integrated Pharmaceutical and Nutritional Sciences, University of Shizuoka, Shizuoka 422-8526, Japan; orcid.org/0000-0002-9937-3100

Shogo Nakano – Graduate School of Integrated Pharmaceutical and Nutritional Sciences, University of Shizuoka, Shizuoka 422-8526, Japan; orcid.org/0000-0002-6614-7158

Complete contact information is available at:
<https://pubs.acs.org/10.1021/acsmchemlett.1c00201>

Author Contributions

#M.T. and Y.T. contributed equally.

Author Contributions

S.Y. and H.K. conceived and designed the project. M.T. and M.W. synthesized compounds. M.T., Y.T., and M.W. analyzed NMR and fluorescence data. M.T. and Y.T. evaluated the fluorescence properties. Y.T. and H.K. performed the docking simulation. M.T. and M.F. performed the fluorescence polarization binding assay. M.K., S.I., and S.N. produced hRXR α -LBD. The manuscript was written by M.T., Y.T., and H.K.

Funding

This work was partially supported by a Grant-in-Aid from the Japan Society for the Promotion of Science (JSPS) 12J06716 (to S.Y.), grants from the Okayama Foundation for Science and Technology (to H.K.), The Tokyo Biochemical Research Foundation (TBRF) (to H.K.), the Kobayashi Foundation (to H.K.), and scholarship support from the Shoshisha Foundation (to Y.T.).

Notes

The authors declare the following competing financial interest(s): This research was partially performed in collaboration with AIBIOS Co., Ltd. M.F. was an employee

of AIBOS. No other author reports any potential conflict of interest relevant to this article.

ACKNOWLEDGMENTS

The authors are grateful to the Division of Instrumental Analysis, Okayama University, for the NMR and MS measurements.

ABBREVIATIONS

BODIPY, boron-dipyrrromethene; COPD, chronic obstructive pulmonary disease; CTCL, cutaneous T-cell lymphoma; Em, emission; Ex, excitation; FITC, fluorescein isothiocyanate; FRET, fluorescence resonance energy transfer; LBP, ligand-binding pocket; LXR, liver X receptor; NBD, nitrobenzoxadiazole; PPAR, peroxisome proliferator-activated receptor; RXR, retinoid X receptor; hRXR α -LBD, human retinoid X receptor α ligand-binding domain; SD, standard deviation; TR, thyroid hormone receptor; Trp, tryptophan; WHO, World Health Organization

REFERENCES

- (1) World Health Organization. *World health Statistics 2020: Monitoring Health for the SDGs, Sustainable Development Goals*. 2020. <https://apps.who.int/iris/handle/10665/332070>.
- (2) Egger, G.; Dixon, J. Beyond Obesity and Lifestyle: a Review of 21st Century Chronic Disease Determinants. *BioMed Res. Int.* **2014**, *2014*, 731685.
- (3) Yamada, S.; Kakuta, H. Retinoid X Receptor Ligands: a Patent Review (2007–2013). *Expert Opin. Ther. Pat.* **2014**, *24*, 443–452.
- (4) Evans, R. M.; Mangelsdorf, D. J. Nuclear Receptors, RXR, and the Big Bang. *Cell* **2014**, *157*, 255–266.
- (5) Germain, P.; Chambon, P.; Eichele, G.; Evans, R. M.; Lazar, M. A.; Leid, M.; De Lera, A. R.; Lotan, R.; Mangelsdorf, D. J.; Gronemeyer, H. International Union of Pharmacology. LXIII. Retinoid X Receptors. *Pharmacol. Rev.* **2006**, *58*, 760–772.
- (6) Mangelsdorf, D. J.; Thummel, C.; Beato, M.; Herrlich, P.; Schütz, G.; Umesono, K.; Blumberg, B.; Kastner, P.; Mark, M.; Chambon, P.; Evans, R. M. The Nuclear Receptor Superfamily: the Second Decade. *Cell* **1995**, *83*, 835–839.
- (7) Forman, B. M.; Umesono, K.; Chen, J.; Evans, R. M. Unique Response Pathways Are Established by Allosteric Interactions among Nuclear Hormone Receptors. *Cell* **1995**, *81*, 541–550.
- (8) Pileri, A.; Delfino, C.; Grandi, V.; Pimpinelli, N. Role of Bexarotene in the Treatment of Cutaneous T-Cell Lymphoma: The Clinical and Immunological Sides. *Immunotherapy* **2013**, *5*, 427–433.
- (9) DeLeon-Pennell, K. Y.; Mouton, A. J.; Ero, O. K.; Ma, Y.; Padmanabhan Iyer, R.; Flynn, E. R.; Espinoza, I.; Musani, S. K.; Vasan, R. S.; Hall, M. E.; Fox, E. R.; Lindsey, M. L. LXR/RXR Signaling and Neutrophil Phenotype Following Myocardial Infarction Classify Sex Differences in Remodeling. *Basic Res. Cardiol.* **2018**, *113*, 40.
- (10) Zuo, Y.; Huang, L.; Enkhjargal, B.; Xu, W.; Umut, O.; Travis, Z. D.; Zhang, G.; Tang, J.; Liu, F.; Zhang, J. H. Activation of Retinoid X Receptor by Bexarotene Attenuates Neuroinflammation Via PPAR- γ /SIRT6/FoxO3a Pathway After Subarachnoid Hemorrhage in Rats. *J. Neuroinflammation* **2019**, *16*, 47.
- (11) Morichika, D.; Miyahara, N.; Fujii, U.; Taniguchi, A.; Oda, N.; Senoo, S.; Kataoka, M.; Tanimoto, M.; Kakuta, H.; Kiura, K.; Maeda, Y.; Kanehiro, A. A Retinoid X Receptor Partial Agonist Attenuates Pulmonary Emphysema and Airway Inflammation. *Respir. Res.* **2019**, *20*, 2.
- (12) Yamauchi, T.; Waki, H.; Kamon, J.; Murakami, K.; Motojima, K.; Komeda, K.; Miki, H.; Kubota, N.; Terauchi, Y.; Tsuchida, A.; Tsuboyama-Kasaoka, N.; Yamauchi, N.; Ide, T.; Hori, W.; Kato, S.; Fukayama, M.; Akanuma, Y.; Ezaki, O.; Itai, A.; Nagai, R.; Kimura, S.; Tobe, K.; Kagechika, H.; Shudo, K.; Kadowaki, T. Inhibition of RXR

and PPAR γ Ameliorates Diet-induced Obesity and Type 2 Diabetes. *J. Clin. Invest.* **2001**, *108*, 1001–1013.

(13) Xia, Y.; Carpentier, A.; Cheng, X.; Block, P. D.; Zhao, Y.; Zhang, Z.; Protzer, U.; Liang, T. J. Human Stem Cell-derived Hepatocytes as a Model for Hepatitis B Virus Infection, Spreading and Virus-host Interactions. *J. Hepatol.* **2017**, *66*, 494–503.

(14) Takahashi, B.; Ohta, K.; Kawachi, E.; Fukasawa, H.; Hashimoto, Y.; Kagechika, H. Novel Retinoid X Receptor Antagonists: Specific Inhibition of Retinoid Synergism in RXR–RAR Heterodimer Actions. *J. Med. Chem.* **2002**, *45*, 3327–3330.

(15) Ebisawa, M.; Umemiya, H.; Ohta, K.; Fukasawa, H.; Kawachi, E.; Christoffel, G.; Gronemeyer, H.; Tsuji, M.; Hashimoto, Y.; Shudo, K.; Kagechika, H. Retinoid X Receptor-Antagonistic Diazepinylbenzoic Acids. *Chem. Pharm. Bull.* **1999**, *47*, 1778–1786.

(16) Yamauchi, T.; Waki, H.; Kamon, J.; Murakami, K.; Motojima, K.; Komeda, K.; Miki, H.; Kubota, N.; Terauchi, Y.; Tsuchida, A.; Tsuboyama-Kasaoka, N.; Yamauchi, N.; Ide, T.; Hori, W.; Kato, S.; Fukayama, M.; Akanuma, Y.; Ezaki, O.; Itai, A.; Nagai, R.; Kimura, S.; Tobe, K.; Kagechika, H.; Shudo, K.; Kadowaki, T. Inhibition of RXR and PPAR γ Ameliorates Diet-Induced Obesity and Type 2 Diabetes. *J. Clin. Invest.* **2001**, *108*, 1001–1013.

(17) Ohsawa, F.; Yamada, S.; Yakushiji, N.; Shinozaki, R.; Nakayama, M.; Kawata, K.; Hagaya, M.; Kobayashi, T.; Kohara, K.; Furusawa, Y.; Fujiwara, C.; Ohta, Y.; Makishima, M.; Naitou, H.; Tai, A.; Yoshikawa, Y.; Yasui, H.; Kakuta, H. Mechanism of Retinoid X Receptor Partial Agonistic Action of 1-(3,5,5,8,8-Pentamethyl-5,6,7,8-Tetrahydro-2-Naphthyl)-1H-Benzotriazole-5-Carboxylic Acid and Structural Development To Increase Potency. *J. Med. Chem.* **2013**, *56*, 1865–1877.

(18) Watanabe, M.; Fujihara, M.; Motoyama, T.; Kawasaki, M.; Yamada, S.; Takamura, Y.; Ito, S.; Makishima, M.; Nakano, S.; Kakuta, H. Discovery of a “Gatekeeper” Antagonist that Blocks Entry Pathway to Retinoid X Receptors (RXRs) without Allosteric Ligand Inhibition in Permissive RXR Heterodimers. *J. Med. Chem.* **2021**, *64*, 430–439.

(19) Yukawa-Takamatsu, K.; Wang, Y.; Watanabe, M.; Takamura, Y.; Fujihara, M.; Nakamura-Nakayama, M.; Yamada, S.; Kikuzawa, S.; Makishima, M.; Kawasaki, M.; Ito, S.; Nakano, S.; Kakuta, H. Convenient Retinoid X Receptor Binding Assay Based on Fluorescence Change of the Antagonist NEt-C343. *J. Med. Chem.* **2021**, *64*, 861–870.

(20) Sajid, A.; Raju, N.; Lusvarghi, S.; Vahedi, S.; Swenson, R. E.; Ambudkar, S. V. Synthesis and Characterization of Bodipy-FL-Cyclosporine A as a Substrate for Multidrug Resistance-Linked P-Glycoprotein (ABC B1). *Drug Metab. Dispos.* **2019**, *47*, 1013–1023.

(21) Thermo Fisher Scientific. Probes for Lipids and Membranes. *Molecular Probes Handbook*, 11th ed., 2010; Chapter 13, pp 544–587.

(22) Fujii, S.; Ohsawa, F.; Yamada, S.; Shinozaki, R.; Fukai, R.; Makishima, M.; Enomoto, S.; Tai, A.; Kakuta, H. Modification at the Acidic Domain of RXR Agonists has Little Effect on Permissive RXR heterodimer Activation. *Bioorg. Med. Chem. Lett.* **2010**, *20*, 5139–5142.

(23) Taniguchi, M.; Lindsey, J. S. Database of Absorption and Fluorescence Spectra of > 300 Common Compounds for Use in PhotochemCAD. *Photochem. Photobiol.* **2018**, *94*, 290–327.

(24) Cheng, L.; Norris, A. W.; Tate, B. F.; Rosenberger, M.; Grippo, J. F.; Li, E. Characterization of the Ligand Binding Domain of Human Retinoid X Receptor α Expressed in Escherichia Coli. *J. Biol. Chem.* **1994**, *269*, 18662–18667.

(25) Birdsall, B.; King, R. W.; Wheeler, M. R.; Lewis, C. A.; Goode, S. R.; Dunlap, R. B.; Roberts, G. C. K. Correction for Light Absorption in Fluorescence Studies of Protein-Ligand Interactions. *Anal. Biochem.* **1983**, *132*, 353–361.

(26) Zhang, H.; Wu, Q.; Berezin, M. Y. Fluorescence Anisotropy (Polarization): from Drug Screening to Precision Medicine. *Expert Opin. Drug Discovery* **2015**, *10*, 1145–1161.

(27) Huang, X.; Aulabaugh, A. Application of Fluorescence Polarization in HTS Assays. *Methods Mol. Biol.* **2016**, *1439*, 115–130.

(28) Lea, W. A.; Simeonov, A. Fluorescence Polarization Assays in Small Molecule Screening. *Expert Opin. Drug Discovery* **2011**, *6*, 17–32.

(29) Trott, O.; Olson, A. J. AutoDock Vina: Improving the Speed and Accuracy of Docking with a New Scoring Function, Efficient Optimization, and Multithreading. *J. Comput. Chem.* **2010**, *31*, 455–461.

(30) Sato, Y.; Ramalanjaona, N.; Huet, T.; Potier, N.; Osz, J.; Antony, P.; Peluso-Iltis, C.; Poussin-Courmontagne, P.; Ennifar, E.; Mely, Y.; Dejaegere, A.; Moras, D.; Rochel, N. The “PhantomEffect” of the Retinoid LG100754: Structural and Functional Insights. *PLoS One* **2010**, *5*, e15119.

(31) Zhang, J. H.; Chung, T. D.; Oldenburg, K. R. A Simple Statistical Parameter for Use in Evaluation and Validation of High Throughput Screening Assays. *J. Biomol. Screening* **1999**, *4*, 67–73.

(32) Huang, X. Fluorescence Polarization Competition Assay: the Range of Resolvable Inhibitor Potency is Limited by the Affinity of the Fluorescent Ligand. *J. Biomol. Screening* **2003**, *8*, 34–38.

(33) Yung-Chi, C.; Prusoff, W. H. Relationship between the Inhibition Constant (K_i) and the Concentration of Inhibitor Which Causes 50% Inhibition (IC_{50}) of an Enzymatic Reaction. *Biochem. Pharmacol.* **1973**, *22*, 3099–3108.